Reconciling Experiment with Quantum Chemical Calculations: Electron Iso-Density Surfaces Represent Atomic and Molecular Surfaces

Amin Alibakhshi[1,*], Lars V. Schäfer[1,*]

[1]Center for Theoretical Chemistry, Ruhr University Bochum, 44780 Bochum, Germany

[*]Email: amin.alibakhshi@ruhr-uni-bochum.de , lars.schaefer@ruhr-uni-bochum.de

Abstract

The surface area of atoms and molecules plays a crucial role in shaping many physiochemical properties of materials. Despite its fundamental importance, precisely defining atomic and molecular surfaces has long been a puzzle. Among the available definitions, a straightforward and elegant approach by Bader describes a molecular surface as an iso-density surface beyond which electron density drops below a certain cut-off. However, so far neither this theory nor a decisive value for the density cut-off have been amenable to experimental verification due to the limitations of conventional experimental methods. In the present study, we employ a state-of-the-art experimental method based on the recently developed concept of thermodynamically effective (TE) surfaces to tackle this longstanding problem. By studying a set of 104 molecules, a close to perfect agreement between quantum chemical evaluations of iso-density surfaces for a cut-off density of 0.0016 a.u. and experimental results obtained via thermodynamic phase change data is demonstrated, with a mean unsigned percentage deviation of 1.6% and a correlation coefficient of 0.995. Accordingly, we suggest the iso-density surface contoured at an electron density value of 0.0016 a.u. as a representation of the surface of atoms and molecules.

Introduction

The molecular surface plays a fundamental role in many physiochemical properties, implying the importance of an accurate characterization of the surfaces of atoms and molecules in a wide range of scientific fields. In a computational context, the molecular surface plays a pivotal role in continuum solvation models [1-3], which are widely used in theoretical and computational chemistry to implicitly include solvent effects, in the study of non-covalent interactions[4-8], van der Waals (vdW) materials [9-12], water-octanol partitioning[13], dispersion interactions in DFT computations [14], thermodynamics of phase changes [15], molecular recognition and reactivity [16-18], crystallization [19], cavity prediction for molecular docking [20, 21], and many other applications.

Investigating atomic and molecular surfaces and their influence on material properties is a topic with a long history. In his pioneering work, Meyer reported already in 1870 a periodic trend in density attributed to the variations in atomic volumes [22]. This seminal work was the cornerstone of conceiving the vdW surfaces and their quantification via crystallography-based experiments by Bragg [23], Pauling [24], Kitaigorodskii [25], and Bondi [26, 27], followed by other experimental methods for estimating vdW surfaces, e.g., via studying the distances of different elements from a probe atom [28], ionization potential [29], thermodynamics of bond breakage [30], and models employing solid molar volumes [31].

Although being insightful and extensively used in many different applications due to the ability to provide a rough estimation of atomic and molecular surfaces, the heuristic definition of the vdW surfaces typically introduces ambiguities. This is reflected in the existence of multiple variants of vdW surfaces, such as solvent-excluded or solvent-accessible ones, as well as multiple parameterizations of atomic radii for them, resulting in a broad range of estimations for molecular

surfaces [15]. The diversity of available parameterizations of atomic vdW radii stems from uncertainties in experimental approaches, which commonly estimate vdW radii from interatomic distances. For crystallography-based experiments, a systematic underestimation of radii is commonly expected due to the stronger interaction between atoms in solids [32-34]. For methods that study atoms in heteronuclear molecules, the estimated radii and resulting surfaces can be affected by bond polarity or anisotropy [35].

Alongside the uncertainties linked to vdW radii parameterization, the construction of molecular vdW surfaces from those radii, due to the assumption of a perfectly spherical shape for the atoms, can also significantly contribute to deviations from the true molecular surfaces. Obviously, for noble gases, the perfect sphere assumption holds and therefore, the vdW surfaces can be a precise representation. Nevertheless, for real molecules, anisotropic distribution of the electron density can result in significant deviations from this assumption. Most importantly, the available parameterizations of vdW radii do not take the dependence of atomic radii on the atomic partial charge into account, which can vary due to the chemical environment.

The above-mentioned limitations in characterizing molecular surfaces can be overcome by an elegant theory initially conceptualized by Bader and co-workers. According to this approach, the surface of atoms and molecules is defined as an iso-density surface beyond which the electron density drops below a certain threshold [36]. Therefore, there is no requirement to parameterize the radii of individual atoms or consider atoms as perfect spheres. Instead, this definition of surfaces only requires electron density data, which can be obtained from quantum chemical computations.

Despite being robust and elegant, the validation of this method and the appropriate cut-off value of the density has not been amenable to extensive experimental verification so far. As a rough

estimate for the cut-off density, Bader and co-workers suggested a value of 0.002 a.u. [36], and Boyd suggested a value of 0.001 a.u. [37], each resulting in significantly different iso-density surfaces. Rahm et al. considered the cut-off density suggested by Boyd for approximating vdW radii of the first 96 elements of the periodic table [38]. One main reason that restricted a more precise quantification of the cut-off density are limitations of experimental methods, as discussed above. Apart from the challenges with experimental methods, constructing the surface of molecules from those radii in a way to properly account for anisotropy in atomic electron densities is not a trivial task.

The recent conception of thermodynamically effective (TE) surfaces [15] now enables to re-examine and benchmark the iso-density definition of molecular surfaces. By suggesting a thermodynamically consistent definition for molecular surfaces, TE surfaces allow an experimental evaluation of molecular surface areas from thermodynamic phase-change data. Importantly, unlike other commonly applied methods that are limited to the evaluation of inter-atomic distances, TE surfaces provide a direct estimate of the total surface area of a molecule, which can then be compared with the iso-density surfaces. Therefore, we select this method in the present study to assess the Bader iso-density theory and to quantify the appropriate value of the density cut-off required in this theory.

Methods

The agreement between TE and iso-density surfaces was benchmarked against the DIPPR database [39]. We only considered compounds in that database for which the reference thermodynamic phase change data of both vaporization enthalpy and surface tension were measured

experimentally and with an uncertainty below 3%, resulting in an initial dataset of 171 compounds. Considering that in the evaluation of TE surfaces, molecules are assumed to follow the ideal gas law in their vapor state [15, 40], we further refined this dataset by excluding molecules that are susceptible to form halogen or hydrogen bonds in the gas phase and thus might significantly deviate from an ideal gas due to cluster formation. Empirical modification of the in-vacuo calculated enthalpies to correct for clustering in the vapor state was demonstrated in a previous study to be necessary for high accuracy estimation of combustion enthalpy [41]. Excluding these compounds yielded a final dataset of 104 compounds, which are listed in the supplementary materials. In addition to from this refined dataset, which serves as the benchmark set in this study, we also evaluated TE and iso-density surfaces for compounds with an uncertainty in the experimental phase change data between 3% and 5%, yielding an additional dataset of 184 compounds. The details of the computed TE and iso-density surfaces for this larger set of compounds is reported in the supplementary materials.

For the studied molecules, experimental values of molecular surface areas (a_s) were obtained by employing the following equation, which describes their relationship to experimental phase-change data of vaporization enthalpy (ΔH_{vap}), surface tension (γ), and critical temperature (T_c)[15]:

$$\Delta H_{vap} = \frac{a_s}{2}\left(2\,\gamma - T\,\frac{d\gamma}{dT}\right) - \frac{RT}{2}\,ln\left(\frac{T}{T_c}\right) \qquad (1)$$

We considered phase-change data at 25 temperature points linearly distributed between the melting point and the critical temperature of each compound and found the a_s values by fitting, as described in Ref. [15]. The temperature dependence of the surface tension and its analytical

derivatives at different temperatures were estimated using the Guggenheim–Katayama relationship [42]:

$$\gamma(T) = \gamma^{\circ}\left(1 - \frac{T}{T_c}\right)^{11/9} \quad (2)$$

The thus obtained molecular surfaces are reported in Table 1.

For the theoretical evaluation of molecular surfaces via the iso-density criterion, we computed the electron densities by ground-state electronic structure computations. Considering that in many molecules, typically multiple low energy conformers contribute to the experimental results, we generated up to 25 low-energy conformers for each molecule using the CREST method [43]. This procedure yielded a total number of 1071 conformers for the 104 studied molecules.

For each conformer, the electron density distribution was acquired via electronic structure computations. For that, the coupled cluster CCSD(T) level of theory is expected to provide the highest accuracy, as this method is considered as the gold standard in quantum chemistry. CCSD(T) calculations generally require large basis sets, and computational costs can be very high. As an alternative, DFT methods can be employed, as they typically provide high accuracy electron densities that may not significantly deviate from the coupled cluster ones despite being obtained at a much lower computational cost. Accordingly, Rahm et al. considered PBE0 computations for evaluating vdW radii based on iso-density surfaces at cut-off density of 0.002 a.u. [38]. In the present study, to acquire accurate electron densities close to complete basis set limit, we first performed electronic structure computations at PBE, B3LYP, DSD-PBEP86 [44], and CCSD(T) levels of theory with the def2-TZVPD basis set. For the DSD-PBEP86 double-hybrid DFT method, which yielded the best agreement with the CCSD(T) computations as demonstrated in the results section below, we re-computed electron densities with the larger def2-QZVPD quadruple-zeta

basis set. The final molecular surfaces were considered as the Boltzmann average of all surfaces computed with the quadruple-zeta basis set for the different conformers of each molecule.

All electronic structure computations were carried out with Orca 5.0.3. [45]. Using the generated wavefunctions for each conformer, total iso-density surfaces were computed for different cut-off densities ranging from 0.0008 to 0.0025 a.u. with 0.0001 a.u. intervals based on an improved marching tetrahedra algorithm [46] developed by Lu and Chen [17] implemented in the Multiwfn software [47].

In addition to the total surface areas of the studied molecules, we also investigated the accuracy of predicted atomic radii of certain elements using TE and iso-density surfaces. For noble gases, where the surfaces are uniquely defined via vdW radii and the perfect sphere assumption holds, estimation of atomic radii from the evaluated TE or iso-density surface is straightforward. For other elements, to avoid undesired effects due to bond polarity, anisotropy, or the radii dependence on atomic partial charges, we only considered homonuclear diatomic molecules N_2, O_2, and F_2 for which phase change data at different temperatures are available in the NIST database [48]. For these molecules, using reference bond lengths taken from the NIST database and the evaluation of the total surface area of the molecule, atomic radii can be estimated using simple geometrical considerations (see supplementary materials for details). We did not consider He, Ne, and H_2 in this analysis, because due to their very low boiling points (below -246 ºC), high uncertainties in thermodynamic phase-change data (and thus in the resulting TE surfaces) are expected.

The agreement between the theoretically estimated molecular surfaces in comparison to the experimental values is reported in terms of mean unsigned percentage error (MUPE) and Pearson correlation coefficient (R),

$$\mathrm{MUPE} = \frac{1}{\mathrm{N}} \sum \left(\left| \frac{y_{i,1} - y_{i,2}}{y_{i,1}} \right| \right) \times 100 \quad (3)$$

$$\mathrm{R} = \frac{\sum (y_{i,1} - \overline{y_1})(y_{i,2} - \overline{y_2})}{\sqrt{\sum (y_{i,1} - \overline{y_1})^2 \sum (y_{i,2} - \overline{y_2})^2}} \quad (4)$$

where $y_{i,1}$ and $y_{i,2}$ are iso-density and TE surfaces of molecule i, respectively, and $\overline{y_1}$ and $\overline{y_2}$ are the corresponding sample means. For the homonuclear diatomic molecules, details of the studied phase change data are provided in the supplementary materials, together with Orca and Multiwfn scripts to calculate iso-density surfaces.

Results and Discussion

The first aim was to identify the DFT method that yields the most accurate electron densities, and to employ it for computations with a larger basis set. Therefore, the iso-density surfaces computed using different DFT methods were compared with those from CCSD(T) computations for the def2-TZVPD basis set. By comparing all DFT iso-density surfaces for all studied cut-off densities (from 0.0008 to 0.0025 a.u., with 0.0001 a.u. intervals) with the respective CCSD(T) iso-density surfaces, we found the best agreement for the double-hybrid DSD-PBEP86 functional showing only 0.08% average absolute deviation (Table 1).

Table 1- Agreement of DFT iso-density surfaces with CCSD(T) results calculated for all studied cut-off densities using the def2-TZVPD basis set. The mean unsigned percentage error (MUPE) and Pearson correlation coefficient (R) are given.

Method	MUPE (%)	R
PBE	0.24	0.9998
B3LYP	0.36	0.9998
DSD-PBEP86	0.08	0.9999

Accordingly, we selected this double-hybrid functional for computations of iso-density surfaces with the larger quadruple-zeta basis set and refer to these DSD-PBEP86/def2-QZVPD calculations in the rest of this study for investigating iso-density surfaces. As a further verification, we also computed iso-density surfaces at the CCSD(T)/def2-QZVPD level of theory, which due to the computational demands could be completed for the lowest energy conformers of a subset of 27 compounds. For them, a comparison of iso-density surfaces between DSD-PBEP86 and CCSD(T) methods, both with the def2-QZVPD basis set, yielded a MUPE of 0.16% and a correlation coefficient of 0.99999, underlining the robustness of the double-hybrid DFT results.

Comparing the theoretically calculated iso-density surfaces (at DSD-PBEP86/def2-QZVPD level of theory) with experimentally derived TE surfaces as reference values for the 104 studied molecules, the best agreement was observed for the cut-off density of 0.0016 a.u., which yielded MUPE and Pearson correlation coefficient of 1.59% and 0.995, respectively. Details of the computed surfaces are provided in the supplementary material.

To further investigate the robustness of this suggested value of the cut-off density, we also evaluated the optimum cut-off densities for 10 datasets, each containing 50 randomly selected compounds from the benchmark set. For all cases, we found the same optimum value of 0.0016 a.u. to yield the best agreement between TE and iso-density surfaces.

Furthermore, for the large dataset containing 184 additional compounds with higher uncertainty in the experimental phase change data, the best agreement between TE and iso-density surfaces was observed for electron density cut-off of 0.0015 a.u. with a MUPE of 6.5%. This result was close to the MUPE of 6.6% obtained using a cut-off density of 0.0016 a.u. (Pearson correlation coefficient is 0.94 in both cases). Despite the larger experimental uncertainties for this dataset, the agreement between the found optimum cut-off densities for the benchmark set and the test set is

very comparable. We thus interpret these results as an additional support of the robustness of the suggested cut-off density of 0.0016 a.u.

Figure 1 shows the agreement of the molecular iso-density surfaces with the TE surfaces as a function of the density cut-off. Density cut-offs in the range 0.0015 – 0.0019 a.u. provide the most accurate results, with an optimum at 0.0016 a.u. The cut-off densities of 0.002 proposed by Bader and co-workers [36] and 0.001 a.u. by Boyd [37] yield MUPEs of 3.17% and 6.98%, respectively, showing the impact of the cut-off density on the computed surfaces and their agreement with the experimental values.

Figure 2 shows correlation plots of the molecular surfaces obtained via the two different approaches, experimentally derived (TE) and iso-density surfaces from DSD-PBEP86/def2-QZVPD computations. Different iso-density surfaces are shown, with cut-off densities of 0.0016 a.u. suggested by us (upper panel), 0.002 a.u. as suggested by Bader (middle panel), and 0.001 a.u. as suggested by Boyd (lower panel). The cut-off density of 0.0016 a.u. provides the best agreement, while the two other cut-off densities applied yield slightly larger deviations. The close to perfect correlation ($R = 0.995$) for all density cut-offs applied underlines the close correspondence between the TE and iso-density surfaces. Considering that the employed experimental TE approach for quantifying molecular surfaces is based on thermodynamic phase-change data while the theoretical results are obtained from the computed electron densities and thus in a completely different way, this remarkable agreement is interpreted as a strong mutual validation of both approaches.

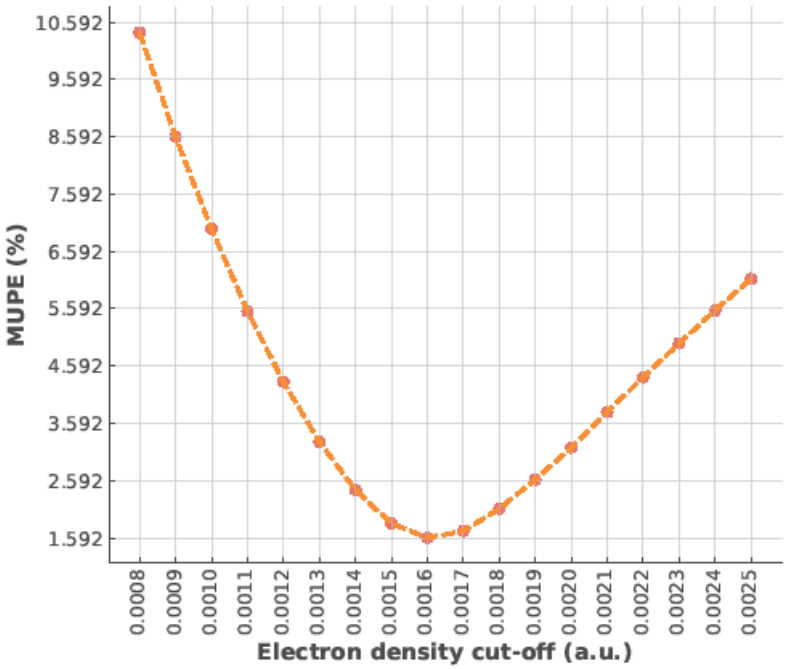

Figure 1- Agreement of computed iso-density surfaces with experimental results TE surfaces as a function of density cut-off

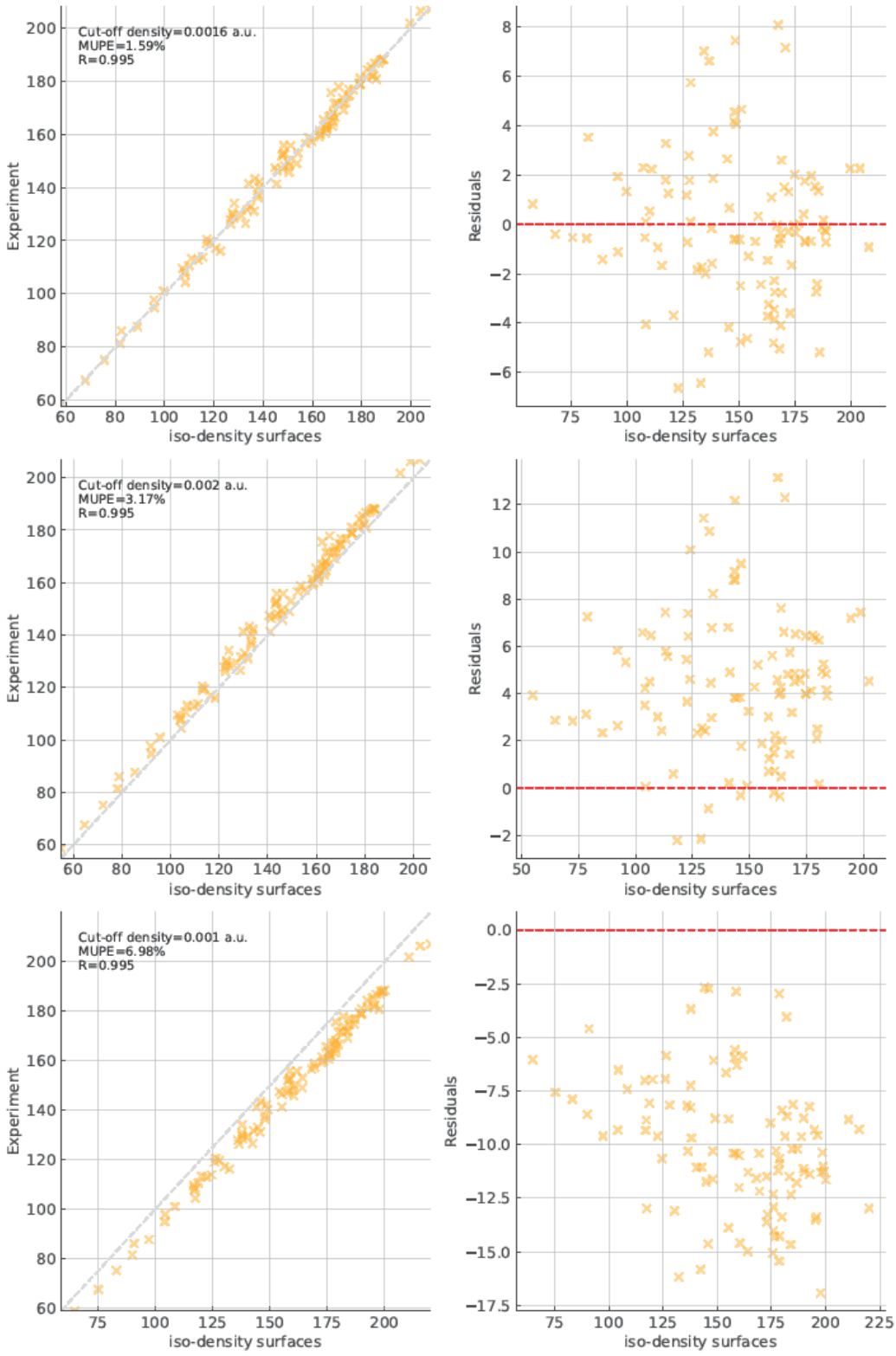

Figure 2 - Comparison of iso-density surfaces from quantum chemical calculations with experimentally derived TE surfaces. Surfaces are in $Å^2$ units.

Further analysis of the results demonstrates the importance of conformer sampling and Boltzmann averaging. When considering only the single lowest-energy conformer of each molecule, the best results were obtained again for the cut-off density of 0.0016 a.u., but the agreement to the TE surfaces (MUPE of 1.87%) was lower than those obtained via conformer sampling (MUPE of 1.59%). The importance of conformer sampling becomes more evident when studying larger and more flexible molecules, which have a greater number of low-energy conformers. Accordingly, in the studied set of molecules, the three most pronounced improvements by conformer sampling were observed for 2-methyl-octane, heptane, and 1-hexanethiol, where the agreement with TE surfaces for single lowest-energy conformers in terms of MUPE were reduced via conformer sampling (Boltzmann averaging) from of 2.30, 4.21, and 2.9 % to 0.44, 2.12, and 0.19 %, respectively. An illustration of the importance of Boltzmann averaging and variation of iso-density surfaces for two low-energy conformers is depicted in Figure 3 for 1-pentanethiol as an example.

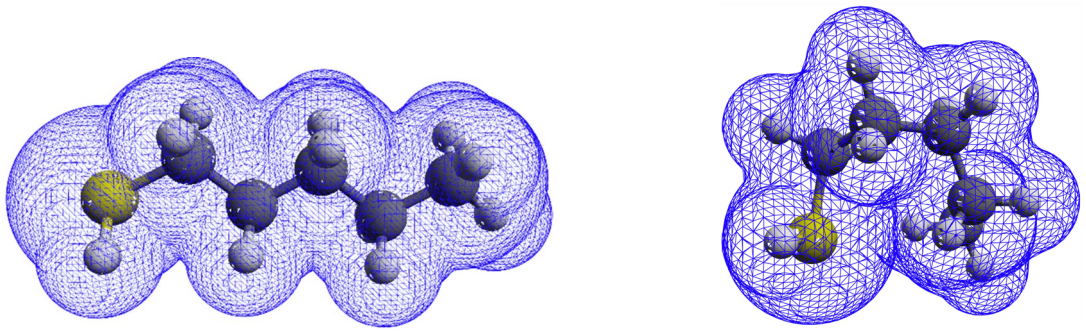

Figure 3- Iso-density surfaces contoured at cut-off density of 0.0016 a.u. computed for two low-energy conformers of 1-pentanethiol. The surface areas of 159.81 Å^2 (left) and 149.21 Å^2 (right) are significantly different from the experimentally determined (TE) surface (156.51 Å^2). The Boltzmann average of iso-density surfaces for multiple conformers of this molecules is 157.20 Å^2, in good agreement with the experimental value.

One of the important applications of the proposed method is the evaluation of atomic radii of elements. In Table 2, we present the atomic radii of a number of elements and their comparison

with experimental estimations. Details of the computations, including employed phase change data are provided in supplementary material.

Table 2- Comparison of different estimations of atomic radii of selected elements (in Å). Experimental estimations of atomic radii for noble gas atoms are taken from Ref. [49] and for other elements from Ref. [28].

	TE	Exp.	iso-density (cut-off 0.0016 a.u.)	iso-density (cut-off 0.001 a.u.)	iso-density (cut-off 0.002 a.u.)
Ar	1.92	1.94	1.87	1.98	1.81
Kr	2.04	2.07	2.01	2.13	1.96
Xe	2.23	2.28	2.20	2.33	2.14
N	1.76	1.66	1.69	1.79	1.64
O	1.60	1.50	1.61	1.71	1.56
F	1.50	1.46	1.52	1.61	1.48

Table 2 shows that for noble gases (for which the uncertainty in experimental estimations are significantly lower, as discussed above), there is an excellent agreement between the atomic radii estimated via TE surfaces, iso-density surfaces with cut-off density of 0.0016 a.u., and reference values from Ref. [49]. Also, for N and F elements, a close agreement between the radii determined via iso-density surfaces and the experimental estimation is observable. For the radii estimated with iso-density cut-off of 0.001 a.u., the results closely match the values reported by Rahm et al. calculated for the same cut-off density at PBE0 level of theory [38]. However, the computed radii with cut-off density of 0.001 a.u. are significantly larger than those predicted by the other studied methods, highlighting the importance of the applied density cut-off. Noteworthy, the estimations of atomic radii for N, O, and F elements via iso-density surfaces are obtained from the diatomic molecule. In another study [50], we recently proposed a rigorous approach to estimate radii of open-shell atoms in their isolated states based on a method proposed by Tkatchenko and Scheffler [14] relating radii of atoms in molecules to the radii of free atoms via:

$$R_A = R_{A,free}\left(\frac{V_A^{eff}}{V_A^{free}}\right)^{1/3}, \quad (5)$$

$$\frac{V_A^{eff}}{V_A^{free}} = \frac{\int r^3 w_A(r) n(r) d^3(r)}{\int r^3 n_A^{free}(r) d^3(r)}, \quad (6)$$

where w_A is the atomic weight for partitioning the molecular space into atomic sub-spaces, and $R_{A,free}$ and n_A^{free} are the radius and the electron density of atom *A* in the free (isolated) state.

Using iso-density surfaces with a cut-off density of 0.0016 a.u., we optimized the radii of free atoms in a way to obtain the best match between solvent-excluded surfaces (SES) constructed via radii of atoms in molecules based on Eq. (5) and iso-density surfaces for a large set of 1235 molecules. The molecular surfaces predicted based on these two different approaches closely matched, with a MUPE of 0.75% and Pearson correlation coefficient of 0.9996. Also, the optimized radii of N and O atoms, found to be 1.65 Å and 1.49 Å, respectively, perfectly agree with the experimental estimations (1.66 Å and 1.50 Å, Table 2). The consistency of the two alternative computational methods for evaluating molecular surfaces and the agreement of the optimized radii with the experimental estimations strongly reinforce the robustness of the proposed approaches.

Conclusions

In the present study, we used quantum chemistry calculations to compute iso-density surfaces for 104 molecules and compared them with accurate experimental estimations based on TE surfaces. Our results show a close agreement between iso-density surfaces for a cut-off density of 0.0016 a.u. and TE surfaces derived from experimental phase-change data with MUPE of 1.59% and correlation coefficient of 0.995. The suggested cut-off density accurately reproduces Bondi radii

of noble gases. Based on these results, we conclude that an iso-density surface around atoms and molecules contoured at an electron density value of 0.0016 a.u. reliably represents atomic and molecular surfaces.

Acknowledgements

This work was supported by the Deutsche Forschungsgemeinschaft (DFG) under Germany's Excellence Strategy - EXC 2033 - 390677874 - RESOLV. We gratefully acknowledge the funding of this project by computing time provided by the Paderborn Center for Parallel Computing (PC2).

Author contributions

AA has conceived and designed this study, carried out the computations, contributed in analysis and interpretation of the data, and wrote the first draft of this manuscript which was then edited by both authors jointly. LVS contributed to analysis and interpretation of the data and writing the manuscript.

Data availability

All data produced in this study are available and can be provided by contacting the corresponding author.

Code availability

The sample code to carry out the computations of TE and iso-density surfaces is provided as supplementary materials.

References:

1. Alibakhshi, A. and B. Hartke, *Implicitly perturbed Hamiltonian as a class of versatile and general-purpose molecular representations for machine learning.* Nature Communications, 2022. **13**(1): p. 1245.
2. Herbert, J.M., *Dielectric continuum methods for quantum chemistry.* Wiley Interdisciplinary Reviews: Computational Molecular Science, 2021. **11**(4): p. e1519.
3. Alibakhshi, A. and B. Hartke, *Improved prediction of solvation free energies by machine-learning polarizable continuum solvation model.* Nature Communications, 2021. **12**(1): p. 1-7.
4. Hu, X., M.-O. Lenz-Himmer, and C. Baldauf, *Better force fields start with better data: A data set of cation dipeptide interactions.* Scientific Data, 2022. **9**(1): p. 327.
5. Visscher, K.M. and D.P. Geerke, *Deriving a polarizable force field for biomolecular building blocks with minimal empirical calibration.* The Journal of Physical Chemistry B, 2020. **124**(9): p. 1628-1636.
6. Murray, J.S. and P. Politzer, *Statistical analysis of the molecular surface electrostatic potential: an approach to describing noncovalent interactions in condensed phases.* Journal of Molecular Structure: THEOCHEM, 1998. **425**(1-2): p. 107-114.
7. Murray, J.S., et al., *Statistically-based interaction indices derived from molecular surface electrostatic potentials: a general interaction properties function (GIPF).* Journal of Molecular Structure: THEOCHEM, 1994. **307**: p. 55-64.
8. Allinger, N.L., X. Zhou, and J. Bergsma, *Molecular mechanics parameters.* Journal of Molecular Structure: THEOCHEM, 1994. **312**(1): p. 69-83.
9. Nallasani, U.R., et al., *Structural and surface characterizations of 2D β-In2Se3/3D β-Ga2O3 heterostructures grown on c-Sapphire substrates by molecular beam epitaxy.* Scientific Reports, 2024. **14**(1): p. 5146.
10. Valadkhani, M., et al., *Curvature and van der Waals interface effects on thermal transport in carbon nanotube bundles.* Scientific Reports, 2022. **12**(1): p. 19531.
11. Liu, Y., et al., *Helical van der Waals crystals with discretized Eshelby twist.* Nature, 2019. **570**(7761): p. 358-362.
12. Liu, Y., Y. Huang, and X. Duan, *Van der Waals integration before and beyond two-dimensional materials.* Nature, 2019. **567**(7748): p. 323-333.
13. Brinck, T., J.S. Murray, and P. Politzer, *Octanol/water partition coefficients expressed in terms of solute molecular surface areas and electrostatic potentials.* The Journal of Organic Chemistry, 1993. **58**(25): p. 7070-7073.
14. Tkatchenko, A. and M. Scheffler, *Accurate molecular van der Waals interactions from ground-state electron density and free-atom reference data.* Physical review letters, 2009. **102**(7): p. 073005.
15. Alibakhshi, A. and B. Hartke, *Dependence of Vaporization Enthalpy on Molecular Surfaces and Temperature: Thermodynamically Effective Molecular Surfaces.* Physical Review Letters, 2022. **129**(20): p. 206001.
16. Spronk, S.A., et al., *A quantum chemical interaction energy dataset for accurately modeling protein-ligand interactions.* Scientific Data, 2023. **10**(1): p. 619.

17. Lu, T. and F. Chen, *Quantitative analysis of molecular surface based on improved Marching Tetrahedra algorithm.* Journal of Molecular Graphics and Modelling, 2012. **38**: p. 314-323.
18. Murray, J.S. and P. Politzer, *The electrostatic potential: an overview.* Wiley Interdisciplinary Reviews: Computational Molecular Science, 2011. **1**(2): p. 153-163.
19. Tong, J., et al., *Crystallization of molecular layers produced under confinement onto a surface.* Nature Communications, 2024. **15**(1): p. 2015.
20. Meng, X.-Y., et al., *Molecular docking: a powerful approach for structure-based drug discovery.* Current computer-aided drug design, 2011. **7**(2): p. 146-157.
21. Thomsen, R. and M.H. Christensen, *MolDock: a new technique for high-accuracy molecular docking.* Journal of medicinal chemistry, 2006. **49**(11): p. 3315-3321.
22. Meyer, L., *Die natur der chemischen elemente als function ihrer atomgewichte*. 1870.
23. Bragg, W.L., *XVIII. The arrangement of atoms in crystals.* The London, Edinburgh, and Dublin Philosophical Magazine and Journal of Science, 1920. **40**(236): p. 169-189.
24. Pauling, L., *The nature of the chemical bond: and the structure of molecules and crystals; an introduction to modern structural chemistry*. 1940.
25. Kitaigorodskii, A., *Organic Crystal Chemistry.* Izd. Akad. Nauk SSSR, Moscow, 1955: p. 15.
26. Bondi, A.v., *van der Waals volumes and radii.* The Journal of physical chemistry, 1964. **68**(3): p. 441-451.
27. Bondi, A., *Van der Waals volumes and radii of metals in covalent compounds.* The Journal of Physical Chemistry, 1966. **70**(9): p. 3006-3007.
28. Alvarez, S., *A cartography of the van der Waals territories.* Dalton Transactions, 2013. **42**(24): p. 8617-8636.
29. Islam, N. and D. C Ghosh, *Spectroscopic evaluation of the atomic size.* The Open Spectroscopy Journal, 2011. **5**(1).
30. Batsanov, S.S., *Thermodynamic determination of van der Waals radii of metals.* Journal of Molecular Structure, 2011. **990**(1-3): p. 63-66.
31. Ben-Amotz, D. and D.R. Herschbach, *Estimation of effective diameters for molecular fluids.* Journal of Physical Chemistry, 1990. **94**(3): p. 1038-1047.
32. Allinger, N., *Calculation of molecular structure and energy by force-field methods*, in *Advances in physical organic chemistry*. 1976, Elsevier. p. 1-82.
33. Zefirov, Y.V. and P. Zorkii, *Van der Waals radii and their application in chemistry.* Russian Chemical Reviews, 1989. **58**(5): p. 421.
34. Naka, T., et al., *Atomic Radii for Depicting Atoms in a Molecule: Cu in Inert Gas Matrix.* Bulletin of the Chemical Society of Japan, 2010. **83**(7): p. 782-787.
35. Batsanov, S.S., *Van der Waals radii of elements.* Inorganic materials, 2001. **37**(9): p. 871-885.
36. Bader, R., W.H. Henneker, and P.E. Cade, *Molecular charge distributions and chemical binding.* The Journal of Chemical Physics, 1967. **46**(9): p. 3341-3363.
37. Boyd, R., *Relative sizes of atoms.[Density contour, scaling].* J. Plasma Phys.;(United Kingdom), 1977. **10**(12).
38. Rahm, M., R. Hoffmann, and N. Ashcroft, *Atomic and ionic radii of elements 1–96.* Chemistry–A European Journal, 2016. **22**(41): p. 14625-14632.
39. Wilding, W.V., R.L. Rowley, and J.L. Oscarson, *DIPPR® Project 801 evaluated process design data.* Fluid phase equilibria, 1998. **150**: p. 413-420.
40. Alibakhshi, A., *Enthalpy of vaporization, its temperature dependence and correlation with surface tension: a theoretical approach.* Fluid Phase Equilibria, 2017. **432**: p. 62-69.
41. Alibakhshi, A. and L.V. Schäfer, *Accurate evaluation of combustion enthalpy by ab-initio computations.* Scientific Reports, 2022. **12**(1): p. 5834.
42. Adam, N., *he physics and chemistry of surfaces (3d ed.): Oxford University Press*. 1941, London.

43. Pracht, P., F. Bohle, and S. Grimme, *Automated exploration of the low-energy chemical space with fast quantum chemical methods.* Physical Chemistry Chemical Physics, 2020. **22**(14): p. 7169-7192.
44. Kozuch, S. and J.M. Martin, *DSD-PBEP86: in search of the best double-hybrid DFT with spin-component scaled MP2 and dispersion corrections.* Physical Chemistry Chemical Physics, 2011. **13**(45): p. 20104-20107.
45. Neese, F., *The ORCA program system.* Wiley Interdisciplinary Reviews: Computational Molecular Science, 2012. **2**(1): p. 73-78.
46. Bulat, F.A., et al., *Quantitative analysis of molecular surfaces: areas, volumes, electrostatic potentials and average local ionization energies.* Journal of molecular modeling, 2010. **16**: p. 1679-1691.
47. Lu, T. and F. Chen, *Multiwfn: A multifunctional wavefunction analyzer.* Journal of computational chemistry, 2012. **33**(5): p. 580-592.
48. Lemmon, E.W., M.L. Huber, and M.O. McLinden, *NIST standard reference database 23.* Reference fluid thermodynamic and transport properties (REFPROP), version, 2010. **9**.
49. Vogt, J.r. and S. Alvarez, *van der Waals radii of noble gases.* Inorganic chemistry, 2014. **53**(17): p. 9260-9266.
50. Alibakhshi A, S.L., *Theoretical Evaluation of Radii of Atoms in Molecules and their Dependence on Atomic Partial Charge.* ChemRxiv, 2024,DOI: 10.26434/chemrxiv-2024-5qz9b.